

Optical studies of charge carrier transport in graphene

Brian A. Ruzicka¹, Shuai Wang², Lalani K. Werake¹, Ben Weintrub¹, Kian Ping Loh², and Hui Zhao^{1*}

¹*Department of Physics and Astronomy, The University of Kansas, Lawrence, Kansas 66045, USA*

²*Department of Chemistry, National University of Singapore, 3 Science Drive 3, Singapore 117543*

**Corresponding Author (Email: huizhao@ku.edu)*

Diffusion of charge carriers in epitaxial graphene and reduced graphene oxide samples are studied using high-resolution optical pump-probe techniques. Spatiotemporal dynamics of carriers after a point-like excitation are monitored. Carrier diffusion coefficients of 11,000 and 5,500 squared centimeters per second are measured in epitaxial graphene and reduced graphene oxide samples, respectively, which are independent of sample temperature in the range from 10 to 300 K. The demonstrated optical techniques can be used for non-contact and non-invasive in-situ detection of transport properties of graphene.

Since its discovery in 2004,[1] graphene, a single layer of carbon atoms, has become one of the most dynamical topics in condensed matter physics, chemistry, and materials science. Owing to the two-dimensional honeycomb-like lattice structure, electrons in graphene behave like Dirac fermions with a linear energy dispersion, described by the relativistic Dirac equation.[2, 3] This opens up possibilities of studying some aspects of high-energy physics in table-top experiments with a condensed matter system. In addition, the strong carbon-carbon covalent bonds make the graphene lattice almost free of defects and impurities. The demonstrated superior properties of graphene include, so far, high carrier mobility at room temperature,[1, 4, 5] high thermal conductivity,[6] and high mechanical strength.[7] These properties make graphene a very attractive candidate for applications like transistors,[1, 8] solar cells,[9] electromechanical resonators,[10], ultracapacitors,[11] and composite materials.[12]

Among these properties, charge transport is the most extensively studied one since it is the foundation of most applications. Previous transport studies, based on electric detection techniques, focused on drift of electrons under an electric field, which is described by the mobility.[1, 4, 5, 8, 13–21] Significant progress has been made in these studies, with demonstrations of ultrahigh mobilities at room temperature,[1, 4, 5] anomalous quantum Hall effects,[4, 5, 22, 23] and a conductivity without charge carriers.[4] In contrast, however, the other aspect of charge transport, carrier diffusion driven by a density gradient, has not been directly studied experimentally. Such a process has played a crucial role in the development of modern semiconductor technology, as it exists in most devices and is utilized in many designs.[24] Furthermore, study of diffusive transport is of fundamental importance since the diffusion coefficient is well related to microscopic quantities such as the mean-free path and scattering rate, that are of great importance in the understanding of interactions between electrons and phonons.

In this Letter, we report the first optical studies of diffusive transport of charge carriers in two types of graphene samples. Using a high-resolution optical pump-

probe technique, a point-like carrier profile is excited by a tightly focused ultrafast laser pulse through interband excitation. Expansion of this carrier profile is monitored by measuring differential transmission of a time-delayed and spatially scanned probe pulse. Carrier diffusion coefficients of 11,000 and 5,500 cm² s⁻¹ are measured in epitaxial graphene and reduced graphene oxide samples, respectively, which are independent of sample temperature in the range from 10 to 300 K. These values are more than two orders of magnitude higher than those of silicon. The measured diffusion coefficients are also compared with previously reported mobilities. Furthermore, the demonstrated optical techniques can be used for non-contact and non-invasive in-situ detection of transport properties of graphene.

We choose two types of graphene samples for our study that are both of great technological relevance, epitaxial graphene and reduced graphene oxide. The former has great potentials to be used in semiconductor industry since it can be produced on large scales with a high degree of repeatability on a insulating substrate,[13] while the latter can be produced with low cost.[20] The epitaxial graphene sample was prepared on a Si-terminated 6H-SiC (0001) crystalline wafer surface by solid-state graphitization.[25, 26] The reduced graphene oxide sample is fabricated by spin coating graphene oxide flakes on a quartz substrate to form a film, which was then transformed to a graphene film by thermal reduction at 1,000°C. By using an atomic force microscope and a scanning tunneling microscope, we determine that the epitaxial sample has one or two layers of graphene, and the reduced oxide graphene sample contains about 50 layers.

The experimental approach for the optical study of carrier transport is rather straightforward. Carriers are first excited with a pump laser pulse that is incident normal to the graphene layer, with a central wavelength of 750 nm, a pulse width of 100 fs, and a spot size of 1.6 μm at full width at half maximum (FWHM), as illustrated in Fig. 1A. The spatial density profile of excited carriers is initially thin, but after a short time, the carriers diffuse out of the excitation spot, which results in a broadening

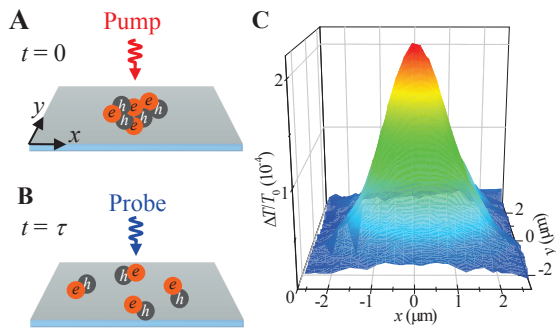


FIG. 1. A: A tightly focused pump laser pulse injects charge carriers in a graphene sample by exciting electrons (e) to the conduction band, leaving holes (h) in the valance band. (B) After a certain period of time, the injected carriers have diffused away from the excitation spot. The expanded carrier density profile is detected by a tightly focused probe pulse. (C) Spatial distribution of the differential transmission signal measured with the probe pulse arriving 0.08 ps after the pump pulse, on the epitaxial graphene sample at room temperature with an injected areal carrier density of 10^{13} cm^{-2} at the center of the excitation spot.

of the profile (Fig. 1B). In this process, electrons (e) and holes (h) move as pairs due to the Coulomb attraction between them. For a classical diffusion process with a Gaussian initial profile, $w^2(t_2) - w^2(t_1) = 16 \ln(2) D (t_2 - t_1)$, where $w(t_2)$ and $w(t_1)$ are the widths (in FWHM) of the profile at two instances of time, and D is the diffusion coefficient. Therefore, by measuring w as a function of time, we can deduce D .

We monitor the diffusion process by using a time-delayed probe pulse with a central wavelength of 810 nm, a pulse width of 190 fs, and a spot size of $1.2 \mu\text{m}$. We verified that under our experimental conditions, the differential transmission of the probe pulse, $\Delta T/T_0 \equiv [T(n) - T_0]/T_0$, i.e. the normalized difference in transmission of the probe with $[T(n)]$ and without (T_0) carriers, is proportional to the carrier density, n . Lock-in detection and balanced detection are both used in order to achieve a high signal-to-noise ratio.[27] Figure 1C shows the spatial profile of $\Delta T/T_0$ measured in the epitaxial graphene sample at room temperature with the probe pulse arriving 0.08 ps after the pump pulse, as we scan the probe spot in the xy plane. With a peak energy fluence of the pump pulse of $170 \mu\text{J cm}^{-2}$, the peak areal carrier density is estimated to be 10^{13} cm^{-2} . The Gaussian shape of the profile is consistent with the laser spots.

To quantitatively study the diffusion process, we measure the profiles along the \hat{x} axis, where the signal is the strongest, for many probe delays, τ . Figure 2A shows an example of the results of such scans. At each x , the $\Delta T/T_0$ decays rapidly with time. The red curve in Fig. 2B (left axis) shows a cross section of Fig. 2A at $x = 0$. Such a fast decay is consistent with the follow-

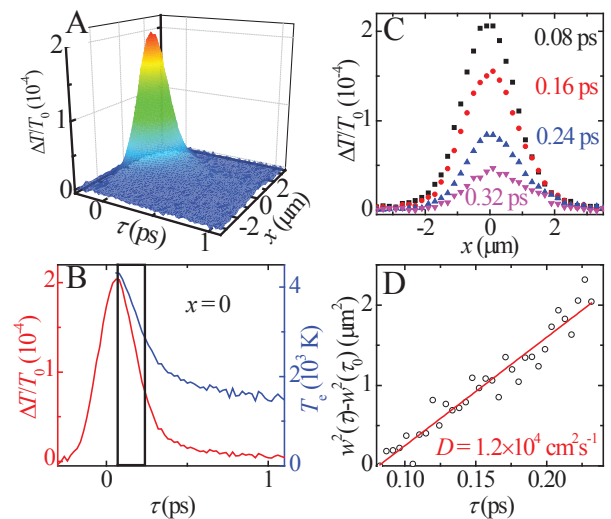


FIG. 2. A: The differential transmission signal as functions of the position of the probe spot with respect to the pump spot, x , and the delay time of the probe pulse with respect to the pump pulse, τ . B: A cross section of Panel A with a fixed $x = 0$ (red line, left axis) and the deduced carrier temperature, T_e (blue line, right axis). C: Cross sections of Panel A along x for several values of τ . D: The expansion of the squared width of the spatial profile. The solid line is a linear fit corresponding to a diffusion coefficient $D = 1.2 \times 10^4 \text{ cm}^2 \text{ s}^{-1}$.

ing picture of the carrier dynamics that has been established by previous time-integrated pump-probe experiments: After excitation, the carriers quickly reach a hot distribution via carrier-carrier scattering within a time scale shorter than 0.1 ps.[28–32] Then, the carriers cool through carrier-phonon scattering on a time scale on the order of 1 ps.[33] The decay of $\Delta T/T_0$ in Fig. 2B is mainly caused by carriers moving out of the detection window of the probe pulse in energy space. From the pump photon energy, we estimate that the initial carrier temperature $T_e \approx 4,300 \text{ K}$. Since $\Delta T/T_0$ is proportional to the density of carriers at the probing energy, we can calculate how T_e changes over time using the measured $\Delta T/T_0$. The result is shown as the blue line in Fig. 2B (right axis).

At all probe delays, the spatial profiles of $\Delta T/T_0$ along x retain a Gaussian shape, with a few examples shown in Fig. 2C. By a gaussian fit to the profile measured at each probe delay in the range from 0.08 to 0.24 ps (indicated as the box in Fig. 2B), we deduce the expansion in the squared width, $w^2(\tau) - w^2(\tau_0)$, where $w(\tau_0)$ is the width of the profile at probe delay $\tau_0 = 0.08 \text{ ps}$, as shown in Fig. 2D. We choose this time range because the $\Delta T/T_0$ signal in this range is large enough for reliable measurements of w . From a linear fit (solid line), we deduce a diffusion coefficient of $D = 1.2 \times 10^4 \text{ cm}^2 \text{ s}^{-1}$. We note that neither the decay of the signal nor the finite size of the probe spot influences the measurement of D : the former does not change the w , and the latter adds a constant, squared width of the probe spot, to the w^2 and

thus does not change the slope.

We use this procedure to systematically investigate the carrier diffusion in both graphene samples. First, at room temperature and at 10 K, no change of the diffusion coefficient was observed when the carrier density is lowered by a factor of five. This indicates that the carrier-carrier scattering does not influence the diffusion process under our experimental conditions. The diffusion coefficient is then measured as a function of the sample temperature in the range of 10 - 300 K. The results are shown in Fig. 3 (left axis) as the solid squares for the epitaxial sample and the solid circles for the reduced graphene oxide sample. At each temperature, multiple measurements were taken at different locations of the samples. The uncertainties on the deduced diffusion coefficient are caused by both the stability of the experimental setup and the inhomogeneity of the samples.

For each sample, the diffusion coefficient does not show a significant dependence on the sample temperature. This is to be expected, however. Immediately after excitation the hot carriers emit a large amount of phonons during the fast energy relaxation process, causing the phonon distribution in the excitation spot to be extremely nonthermal. Since the local phonon distribution is determined by the hot carriers instead of the sample temperature, the environment that the carriers experience is independent of the temperature of the whole sample. By averaging the values measured at all the sample temperatures, we get the diffusion coefficients of $1.1 \times 10^4 \text{cm}^2 \text{s}^{-1}$ for the epitaxial sample and $5.5 \times 10^3 \text{cm}^2 \text{s}^{-1}$ for the reduced graphene oxide sample. These values are significantly higher than silicon, which has an electron (hole) diffusion coefficient of 36 (12) $\text{cm}^2 \text{s}^{-1}$ at room temperature.[24] Furthermore, it is quite encouraging that the charge transport properties of the reduced graphene oxide sample is only a factor of two worse than the epitaxial graphene, since the fabrication of this type of graphene is low cost.[20]

In this optical study, equal numbers of electrons and holes are injected, and therefore the diffusion is ambipolar. The ambipolar diffusion coefficient is related to the unipolar diffusion coefficients of electrons and holes, and is dominated by the lower one.[24] Since the electrons and holes in graphene have the same energy dispersion, the diffusion coefficients for both are expected to be the same. Therefore, the diffusion coefficients we determined are also the unipolar diffusion coefficients of electrons and holes.

For a thermalized system, the diffusion coefficient is related to the mobility, μ , by Einstein relation, $\mu = qD/k_B T_e$, where q and k_B are the amount of charge of each carrier and Boltzmann's constant.[24] Due to the ultrafast thermalization process in graphene,[28–32] the carriers can be treated as a thermalized system. However, the diffusion occurs during the energy relaxation process. During the time range of the measurement, T_e changes

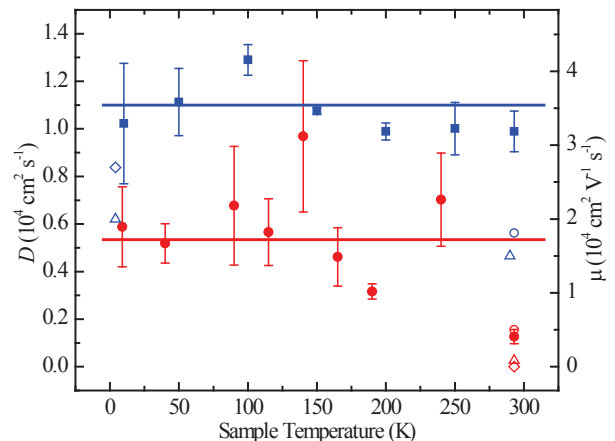


FIG. 3. Diffusion coefficient (D , left axis) as a function of the sample temperature for the epitaxial sample (solid squares) and the reduced graphene oxide sample (solid circles) measured by the procedure summarized in Fig. 2. The mobility (μ , right axis) is deduced by using Einstein relation with a carrier temperature $T_e = 3600$ K. For comparison, previously reported values of mobilities in epitaxial graphene (blue open symbols: the circle from Ref.[14], the triangles from Ref.[15], and the diamond from Ref.[13]) and reduced graphene oxide samples (red open symbols: the circle from Ref.[19], the triangle from Ref.[21], and the diamond from Ref.[20]) are also plotted.

from 4,300 to 2,900 K (Fig. 2B, right axis). To estimate the mobility corresponding to the measured diffusion coefficients, we use an average temperature in this range of 3,600 K. The deduced mobilities are shown in Fig. 3 with the same symbols as the diffusion coefficient, but with the right axis. For the epitaxial graphene sample, we obtain a mobility of $3.5 \times 10^4 \text{cm}^2 \text{V}^{-1} \text{s}^{-1}$. Previous mobility measurements on epitaxial graphene have obtained rather different results.[8, 13–18] However, the highest reported values are typically in the range of 1.5×10^4 to $2.7 \times 10^4 \text{cm}^2 \text{V}^{-1} \text{s}^{-1}$ (blue open symbols in Fig. 3),[13–15] almost independent of sample temperature. Our results are reasonably consistent with these values. For the reduced graphene oxide sample, we deduced a mobility of $1.7 \times 10^4 \text{cm}^2 \text{V}^{-1} \text{s}^{-1}$. Fewer studies on mobility in this type of graphene have been reported; available data are plotted in Fig. 3 as the red open symbols.[19–21] We note that our results at room temperature is consistent with the previous reported values of similar samples prepared with the same procedures.[19]

In summary, we have demonstrated that a spatially resolved ultrafast optical technique can be used to determine the carrier diffusion coefficient in graphene, which is an important quantity describing charge transport that has never been measured before. Compared to electric methods that are widely used to study transport properties of graphene, this optical technique has several advantages. As a non-contacting and non-invasive technique

with high spatial resolution, it can be used for in situ detection of transport properties at different locations of a sample or for direct comparison of multiple samples. Since no electrode is needed, its potential influence on the transport measurement is excluded. Furthermore, by selecting the laser wavelength and the time range of detection, one can study transport of hot carriers with different temperatures and compare transport properties of thermal and nonthermal carrier systems.

HZ acknowledges support from the US National Science Foundation under Awards No. DMR-0954486 and No. EPS-0903806, and matching support from the State of Kansas through Kansas Technology Enterprise Corporation. KPL thanks the support of NRF-CRP "Graphene Related Materials and Devices" (Grant No. R-143-000-360-281).

-
- [1] K. S. Novoselov, A. K. Geim, S. V. Morozov, D. Jiang, Y. Zhang, S. V. Dubonos, I. V. Grigorieva, and A. A. Firsov, *Science* **306**, 666 (2004).
- [2] A. H. C. Neto, F. Guinea, N. M. R. Peres, K. S. Novoselov, and A. K. Geim, *Rev. Mod. Phys.* **81**, 109 (2009).
- [3] A. K. Geim and K. S. Novoselov, *Nat. Mater.* **6**, 183 (2007).
- [4] K. S. Novoselov, A. K. Geim, S. V. Morozov, D. Jiang, M. I. Katsnelson, I. V. Grigorieva, S. V. Dubonos, and A. A. Firsov, *Nature* **438**, 197 (2005).
- [5] Y. Zhang, Y. W. Tan, H. L. Stormer, and P. Kim, *Nature* **438**, 201 (2005).
- [6] A. A. Balandin, S. Ghosh, W. Bao, I. Calizo, D. Teweldebrhan, F. Miao, and C. N. Lau, *Nano Lett.* **8**, 902 (2008).
- [7] C. Lee, X. Wei, J. W. Kysar, and J. Hone, *Science* **321**, 385 (2008).
- [8] Y. M. Lin, C. Dimitrakopoulos, K. A. Jenkins, D. B. Farmer, H. Y. Chiu, A. Grill, and P. Avouris, *Science* **327**, 662 (2010).
- [9] Z. F. Liu, Q. Liu, Y. Huang, Y. F. Ma, S. G. Yin, X. Y. Zhang, W. Sun, and Y. S. Chen, *Adv. Mater.* **20**, 3924 (2008).
- [10] S. Bunch, A. M. van der Zande, S. S. Verbridge, I. W. Frank, D. M. Tanenbaum, J. M. Parpia, H. G. Craighead, and P. L. McEuen, *Science* **315**, 490 (2007).
- [11] M. D. Stoller, S. Park, Y. Zhu, J. An, and R. S. Ruoff, *Nano Lett.* **8**, 3498 (2008).
- [12] S. Stankovich, D. A. Dikin, G. H. B. Dommett, K. M. Kohlhaas, E. J. Zimney, E. A. Stach, R. D. Piner, S. T. Nguyen, and R. S. Ruoff, *Nature* **442**, 282 (2006).
- [13] C. Berger, Z. Song, X. Li, X. Wu, N. Brown, C. Naud, D. Mayou, T. Li, J. Hass, A. N. Marchenkov, et al., *Science* **312**, 1191 (2006).
- [14] J. A. Robinson, M. Wetherington, J. L. Tedesco, P. M. Campbell, X. Weng, J. Stitt, M. A. Fanton, E. Frantz, D. Snyder, B. L. Vanmil, et al., *Nano Lett.* **9**, 2873 (2009).
- [15] X. S. Wu, Y. K. Hu, M. Ruan, N. K. Madiomanana, J. Hankinson, M. Sprinkle, C. Berger, and W. A. D. Heer, *Appl. Phys. Lett.* **95**, 223108 (2009).
- [16] G. Gu, S. Nie, R. M. Feenstra, R. P. Devaty, W. J. Choyke, W. K. Chan, and M. G. Kane, *Appl. Phys. Lett.* **90**, 253507 (2007).
- [17] K. V. Emtsev, A. Bostwick, K. Horn, J. Jobst, G. L. Kellogg, L. Ley, J. L. Mcchesney, T. Ohta, S. A. Reshanov, J. Rohrl, et al., *Nat. Mater.* **8**, 203 (2009).
- [18] S. Odaka, H. Miyazaki, S. L. Li, A. Kanda, K. Morita, S. Tanaka, Y. Miyata, H. Kataura, K. Tsukagoshi, and Y. Aoyagi, *Appl. Phys. Lett.* **96**, 062111 (2010).
- [19] S. A. Wang, P. K. Ang, Z. Q. Wang, A. L. L. Tang, J. T. L. Thong, and K. P. Loh, *Nano Lett.* **10**, 92 (2010).
- [20] G. Eda, G. Fanchini, and M. Chhowalla, *Nat. Nanotechnol.* **3**, 270 (2008).
- [21] X. S. Wu, M. Sprinkle, X. B. Li, F. Ming, C. Berger, and W. A. de Heer, *Phys. Rev. Lett.* **101**, 026801 (2008).
- [22] Y. Zhang, Y. W. Tan, H. L. Stormer, and P. Kim, *Science* **315**, 1379 (2007).
- [23] K. S. Novoselov, E. McCann, S. V. Morozov, V. I. Fal'ko, M. I. Katsnelson, U. Zeitler, D. Jiang, F. Schedin, and A. K. Geim, *Nat. Phys.* **2**, 177 (2006).
- [24] D. A. Neamen, *Semiconductor physics and devices* (McGraw-Hill, 2002).
- [25] H. Huang, W. Chen, S. Chen, and A. T. S. Wee, *ACS Nano* **2**, 2513 (2008).
- [26] W. Chen, K. P. Loh, H. Xu, and A. T. S. Wee, *Langmuir* **20**, 10779 (2004).
- [27] H. Zhao, E. J. Loren, H. M. van Driel, and A. L. Smirl, *Phys. Rev. Lett.* **96**, 246601 (2006).
- [28] J. M. Dawlaty, S. Shivaraman, M. Chandrashekar, F. Rana, and M. G. Spencer, *Appl. Phys. Lett.* **92**, 042116 (2008).
- [29] D. Sun, Z. K. Wu, C. Divin, X. B. Li, C. Berger, W. A. d. and P. N. First, and T. B. Norris, *Phys. Rev. Lett.* **101**, 157402 (2008).
- [30] P. A. George, J. Strait, J. Dawlaty, S. Shivaraman, M. Chandrashekar, F. Rana, and M. G. Spencer, *Nano Lett.* **8**, 4248 (2008).
- [31] R. W. Newson, J. Dean, B. Schmidt, and H. M. van Driel, *Opt. Exp.* **17**, 2326 (2009).
- [32] S. Kumar, M. Anija, N. Kamaraju, K. S. Vasu, K. S. Subrahmanyam, A. K. Sood, and C. N. R. Rao, *Appl. Phys. Lett.* **95**, 191911 (2009).
- [33] H. Wang, J. H. Strait, P. A. George, S. Shivaraman, V. B. Shields, M. Chandrashekar, J. Hwang, F. Rana, M. G. Spencer, C. S. Ruiz-Vargas, et al., *Appl. Phys. Lett.* **96**, 081917 (2010).